Numerical study of the magnetic skin effect: Efficient parameterization of 2D surface-impedance solutions for linear ferromagnetic materials

Dima Abou El Nasser El Yafi, Victor Péron, Ronan Perrussel, Laurent Krähenbühl

A NUMERICAL STUDY OF THE MAGNETIC SKIN EFFECT: EFFICIENT PARAMETRIZATION OF 2D SURFACE-IMPEDANCE SOLUTION FOR LINEAR FERROMAGNETIC MATERIALS

DIMA ABOU EL NASSER EL YAFI, VICTOR PÉRON, RONAN PERRUSSEL, LAURENT KRÄHENBÜHL

Abstract. This work presents an efficient method based on asymptotic models in order to solve numerically eddy current problems in a bi-dimensional setting with a high contrast of linear relative magnetic permeability $\mu_r \gg 1$ between a conductor and a dielectric subdomain. We describe a magnetic *skin effect* by deriving a multiscale expansion for the magnetic potential in power series of a small parameter δ which represents the skin depth. We make explicit the first asymptotics up to the order three. Some numerical results based on the finite element method will be presented to illustrate the magnetic skin effect and to validate the performance of the proposed asymptotic models in the dielectric medium. We confirm that the proposed asymptotics provide reduced computational costs for a wide range of the physical parameters introduced in our problem.

Keywords. Asymptotic expansions; Impedance boundary conditions; Eddy current problems; Finite element method; Magnetic potential; Ferromagnetic materials.

1. Introduction

For several decades, the eddy current problem has been the interest of an intensive research [12, 13, 14, 10, 6, 4, 3, 2, 19, 20, 17, 8, 16]. Indeed, eddy currents are crucial for the design of industrial systems such as the induction heating or the breaking of heavy vehicles. In contrast, eddy currents may induce "undesirable" losses that affect negatively the performance of some devices for example motors and generators. As a result, studying eddy currents is significant in the engineering applications.

In this context, our interest lies in the numerical solution of the eddy current problem for ferromagnetic materials using an asymptotic approach, in a bi-dimensional setting. In fact, we consider laminated cores in the transformers that are made of magnetic thin sheets coated with an insulating layer and oriented parallel to the magnetic flux, in order to reduce energy losses resulting from the eddy currents. However, eddy currents tend to accumulate near the surface of these materials, this is the so-called skin effect.

More precisely, this effect reflects the rapid decay of the magnetic field inside these ferromagnetic materials. In this paper, we intend to perform a numerical simulation of the magnetic skin effect by applying a finite element method to our problem, on a mesh that combines thin cells inside the skin depth and much larger cells outside this zone. Furthermore, we derive asymptotic models that provide reduced computational costs for a wide range of frequencies, conductivities as well as relative permeabilities.

The problem under consideration lies in two different materials with a common interface Σ: we are interested to study the magnetic potential in a magnetic conducting body with high relative permeability $\mu_r \gg 1$ embedded in a dielectric medium that we consider it for the sake of simplicity the free space. The conductivity σ and the angular frequency ω are given parameters.

The aim of this work is to propose asymptotic models that are validated using a finite element approach with a fine mesh on the interface of the conductor. This numerical approach enables the simulation of the skin effect. Moreover, in order to evaluate the accuracy of the proposed asymptotic solutions, we establish a numerical comparison with the impedance boundary conditions (IBCs) solutions [9, 1, 5, 7] that are among the most crucial methods for solving time-harmonic eddy current problems with a small skin depth denoted by δ. To shed a light on our approach, we emphasize that the IBCs method is not more efficient since the computational costs of the proposed method is less than the IBCs solutions regardless the number of the given physical parameters to be considered.

1.1. **Related works.** In this paper, we employ an asymptotic approach that was previously involved in the context of the eddy current problems for highly conductive non-magnetic materials [13, 9, 15, 11]. More precisely, the solution of the eddy current problems is established previously [13] using a multiscale expansion in a bi-dimensional setting where the domain is considered unbounded and the solution grows logarithmically to infinity. Moreover, authors developed $\delta - parametrization$ in high frequency or high conductivity [9, 15, 11] that derives real asymptotics and family of Dirichlet problems for the Laplace operator set in the dielectric medium. Furthermore, in [9, 11], we observe that the asymptotic models have reduced computational costs since it does not depend on the physical parameters embedded in the eddy current problems. In contrast, our work is motivated by a recent article [17] with its primary focus directed toward theoretical studies of the eddy current problems for magnetically soft materials deduced from asymptotic analysis. We provide numerical experiments in order to validate the performance of the proposed asymptotic models introduced in the $\varepsilon - parametrization$ of the magnetic potential ($\varepsilon = \dfrac{1}{\mu_r \delta} \ll 1$), as well as to illustrate a boundary layer inside the magnetic conductor in a vicinity of its surface i.e. the magnetic skin effect.

Finally, our numerical simulations illustrate that the magnetic field lines penetrate orthogonally to the conductor, contrary to the high conductivity case for which the direction of the magnetic field lines is tangential to the conductor.

1.2. **Organisation of the paper.** The outline of the paper proceeds as follows. Section 2 will present the framework as well as the boundary value problem. In section 3, we exhibit the asymptotic expansion and convergence results. Section 3.2 is devoted to the identification of the asymptotic models up to the order two. In section 4, we present numerical results in order to evaluate the performance of the proposed models. Concluding remarks and perspectives are given in section 5. In appendix A, we provide elements of proof of the multiscale expansion introduced in section 3.1.

2. Problem setting

Let us consider the case of a two dimensional medium Ω with a boundary Γ. Our problem can be formulated as a conducting material $\Omega_- \subset\subset \Omega$ and a dielectric medium Ω_0 considered for the sake of simplicity as the free space, with a common interface Σ, see Fig. 1. We note that, unless specified, all the considered domains are smooth and bounded in $\mathbb{R}^2$.

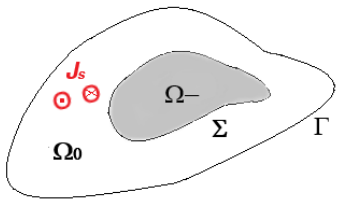

Figure 1. The domain Ω and its subdomains Ω_-, Ω_0

The time harmonic eddy current problem can be written as follows [17]

$$-\nabla.(\frac{1}{\underline{\mu}}\nabla A) + i\omega\underline{\sigma}\mathbb{1}_{\Omega_-} A = J \qquad in \quad \Omega, \tag{1}$$

where A is the magnetic vector potential reduced to a single scalar component in this two dimensional situation, ω is the angular frequency and J represents the current source.

The magnetic permeability and the conductivity are given by the following piecewise-constant functions $\underline{\mu}$ and $\underline{\sigma}$ respectively:

$$\underline{\mu} = \begin{cases} \mu_0 & in \quad \Omega_0 \\ \mu_r\mu_0 & in \quad \Omega_- \end{cases} \qquad and \qquad \underline{\sigma} = \begin{cases} 0 & in \quad \Omega_0 \\ \sigma & in \quad \Omega_-, \end{cases} \tag{2}$$

where $\mu_0 = 4\pi \times 10^{-7}$ [H/m](Henry per meter) and the relative permeability μ_r is assumed to be a large parameter. For the sake of simplicity, we shall

consider that the current source J is a smooth function and the support of J does not meet Ω_-.

2.1. **Notations and parameters.** In order to apply the asymptotic approach, we define a "small" parameter as follows:

$$\varepsilon = \frac{1}{\mu_r \delta},$$

where δ is the skin depth and given by the following formula

$$\delta = \sqrt{\frac{2}{\omega \sigma \mu_0 \mu_r}} \quad .$$

Note that both parameters ε and δ tend to zero when the relative permeability μ_r tends to infinity.

Hereafter, we consider the following notations.

Notation 1. *We denote by h^+ (resp. h^-) the restriction of any function h in Ω_0 (resp.Ω_-).*

2.2. **Boundary value problem.** The magnetic vector potential $A = (A^+, A^-)$ satisfies the following boundary problem

(3)
$$\left\{\begin{array}{ll} -\Delta A^+ = \mu_0 J_s & in\ \Omega_0, \\ -\Delta A^- + i\ \omega\sigma\mu_0\mu_r A^- = 0 & in\ \Omega_-, \\ A^+ = A^- & on\ \Sigma, \\ \partial_n A^+ = \mu_r^{-1} \partial_n A^- & on\ \Sigma, \\ A^+ = 0 & on\ \Gamma, \end{array}\right. \iff \left\{\begin{array}{ll} -\Delta A^+ = \mu_0 J_s & in\ \Omega_0, \\ -\Delta A^- + 2i\delta^{-2} A^- = 0 & in\ \Omega_-, \\ A^+ = A^- & on\ \Sigma, \\ \partial_n A^+ = \varepsilon\delta \partial_n A^- & on\ \Sigma, \\ A^+ = 0 & on\ \Gamma, \end{array}\right.$$

where the differential operator Δ is the Laplace operator in cartesian coordinates $\mathbf{x} = (x, y) \in \mathbb{R}^2$. As a convention, the unit normal vector $\mathbf{n}$ on the interface Σ is inwardly oriented to Ω_-.

3. Multiscale expansion

In order to derive a multiscale expansion for the solution $A = (A^+, A^-)$ of the model problem(3), we assume that Σ is a smooth curve. Then we construct an asymptotic expansion for the solution A as follows:

$$A^+(\mathbf{x}) = A_0^+(\mathbf{x}) + \frac{\varepsilon}{\alpha} A_1^+(\mathbf{x}) + \left(\frac{\varepsilon}{\alpha}\right)^2 A_2^+(\mathbf{x}) + \cdots \qquad in \quad \Omega_0, \tag{4}$$

$$A^-(\mathbf{x}) = \mathcal{U}_0(\xi, \frac{h}{\delta}) + \delta \mathcal{U}_1(\xi, \frac{h}{\delta}) + \delta^2 \mathcal{U}_2(\xi, \frac{h}{\delta}) + \cdots \qquad in \quad \Omega_-. \tag{5}$$

where $\mathcal{U}_j \longrightarrow 0$ as $Y = \frac{h}{\delta} \longrightarrow +\infty, \forall j \in \mathbb{N}$. We note here $\mathbf{x} = (x, y) \in \mathbb{R}^2$ are the cartesian coordinates and $\alpha = \dfrac{1-i}{2}$. In (5) we applied a multiscale

expansion based on a "curvilinear coordinate system" denoted by (ξ, h). More precisely, ξ is a curvilinear abscissa on the interface Σ and h is the distance to this latter curve, see for instance Fig. 2

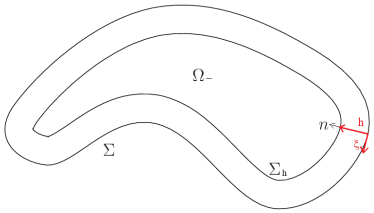

FIGURE 2. A tubular neighborhood of the surface Σ.

3.1. **Convergence result.** Now we validate the asymptotic expansions (4)-(5) by proving estimates for the following reminder r_m defined at any order $m \in \mathbb{N}^*$ as

$$
\begin{aligned}
r^+_{m,\varepsilon} &= A^+ - \sum_{n=0}^{m} \left(\frac{\varepsilon}{\alpha}\right)^n A^+_n \qquad in \quad \Omega_0, \\
r^-_{m,\delta} &= A^- - \sum_{n=0}^{m} \delta^n \mathcal{U}_n(\xi, \frac{h}{\delta}) \qquad in \quad \Omega_-.
\end{aligned} \tag{6}
$$

We introduce the small parameter $\nu = \dfrac{1}{\sqrt{\mu_r}}$ in the theorem below. The proof of the following convergence result is worked out previously [17] (cf theorems (2.3)-(2.4)) in a slightly different configuration.

Theorem 1. *There exists $\nu_0 > 0$ such that for all $m \in \mathbb{N}$ there exists a constant $C_m > 0$ independent of ν such that for all $\nu \in (0, \nu_0)$ the remainder r_m satisfies the optimal estimate*

$$
\|r^+_{m;\varepsilon}\|_{1,\Omega_+} + \nu \|\nabla r^-_{m;\delta}\|_{0,\Omega_-} + \|r^-_{m;\delta}\|_{0,\Omega_-} \leq C_m \nu^{m+1}. \tag{7}
$$

We denote by $\|.\|_{1,\Omega_+}$ the norm in the Sobolev space $\mathrm{H}^1(\Omega_+)$ and $\|.\|_{0,\Omega_-}$ the norm in $\mathrm{L}^2(\Omega_-)$.

We note that this convergence result is *a priori* valid for non smooth domain, as we will see in section 4.3 using numerical illustrations.

3.2. **First terms of the asymptotic expansion.** In this section, we identify the first asymptotics for the multiscale expansion (4)-(5) where j=0,1,2. Elements of formal derivations are given in the appendix A.

We apply the following notations in the expressions of the asymptotics.

Notation 2. *We denote by L the length of the interface Σ. Then we define a smooth function $\boldsymbol{X}$ from $\mathbb{T}_L := \mathbb{R}/L\mathbb{Z}$ into $\mathbb{R}^2$. We note that $\boldsymbol{X}(\xi) \in \Sigma$ is*

an arc length parametrization of Σ. *The scalar curvature* $k(\xi)$ *at the point* $\boldsymbol{X}(\xi)$ *is well-defined by* [17]

$$\frac{d\boldsymbol{n}}{d\xi} = -k(\xi)\frac{d\boldsymbol{X}}{d\xi}.$$

We remind that $\boldsymbol{n}(\xi)$ *denotes the unit normal at* $\boldsymbol{X}(\xi) \in \Sigma$ *which is inwardly oriented to* Ω_-.

Now we construct the first asymptotics $(A_0^+,\mathcal{U}_0),(A_1^+,\mathcal{U}_1)$ and $(A_2^+,\mathcal{U}_2)$ recursively. First, A_0^+ solves the problem:

$$\begin{cases} -\Delta A_0^+ = \mu_0 J, & \text{in } \Omega_0, \\ \partial_n A_0^+ = 0 & \text{on } \Sigma, \\ A_0^+ = 0 & \text{on } \Gamma. \end{cases} \tag{8}$$

We remark that A_0^+ satisfies the perfect magnetic conductor condition. Then the first profile $\mathcal{U}_0$ is defined as follows

$$\mathcal{U}_0(\xi, Y) = A_0^+(\mathbf{X}(\xi))e^{-\frac{Y}{\alpha}}. \tag{9}$$

The next asymptotic A_1^+ solves the problem below

$$\begin{cases} -\Delta A_1^+ = 0, & \text{in } \Omega_0, \\ \partial_n A_1^+ = -A_0^+ & \text{on } \Sigma, \\ A_1^+ = 0 & \text{on } \Gamma. \end{cases} \tag{10}$$

The second profile $\mathcal{U}_1$ satisfies the following equality

$$\mathcal{U}_1(\xi, Y) = \Big(\frac{1}{\alpha\delta_0^2}A_1^+(\mathbf{X}(\xi)) + \frac{k(\xi)}{2}A_0^+(\mathbf{X}(\xi))Y\Big)e^{-\frac{Y}{\alpha}} \tag{11}$$

where $\delta_0 = \sqrt{\dfrac{2}{\omega\sigma\mu_0}}$.

The third asymptotic A_2^+ solves the following problem

$$\begin{cases} -\Delta A_2^+ = 0 & \text{in} \quad \Omega_0, \\ \partial_n A_2^+ = \frac{k(\xi)}{2}A_0^+ - \frac{1}{\alpha^2\delta_0^2}A_1^+ & \text{on} \quad \Sigma, \\ A_2^+ = 0 & \text{on} \quad \Gamma. \end{cases} \tag{12}$$

Finally, the third profile $\mathcal{U}_2$ satisfies the following equality

$$\mathcal{U}_2(\xi, Y) = \left(\left(\frac{1}{\alpha\delta_0^2}\right)^2 A_2^+ + \left(\frac{k(\xi)}{2}\frac{\delta_0}{\alpha}A_1^+ + \frac{\alpha}{2}\left\{\partial_\xi^2 + \frac{k(\xi)^2}{4}\mathbb{I}\right\}A_0^+\right)Y + \frac{3k(\xi)^2}{8}A_0^+Y^2\right)(X(\xi))e^{-\frac{Y}{\alpha}}. \tag{13}$$

The first asymptotics reveal some interesting properties. We note that the first two asymptotics A_0^+ and A_1^+ are real and independent of the physical parameters. Consequently, we can calculate the second approximation $A_0^+ + \frac{\varepsilon}{\alpha}A_1^+$ with reduced computational costs, since in order to identify A_0^+ and A_1^+, we apply the finite element approach only once regardless the number of the physical parameters to be considered. In contrast, we remark that the asymptotic A_2^+ depends on the angular frequency ω and the conductivity σ.

Therefore we need to compute the finite element approach at each time we change the physical parameters in order to identify A_2^+ in the third order approximation $A_0^+ + \frac{\varepsilon}{\alpha}A_1^+ + \left(\frac{\varepsilon}{\alpha}\right)^2 A_2^+$. For this reason, in the next section, our interest lies in the validation of the accuracy of the asymptotic models (8)-(10) using the finite element approach.

4. Numerical results

We now present some numerical results in order to demonstrate the accuracy of our asymptotic models up to the order two in the dielectric medium.

We will first introduce geometrical and physical assumptions. Then we will exhibit the post-processing of the skin effect and the direction of the magnetic field lines. Furthermore, we perform a comparison between the reference solution and the asymptotic solution of order one as well as the corresponding error and its correction. In order to evaluate the precision of

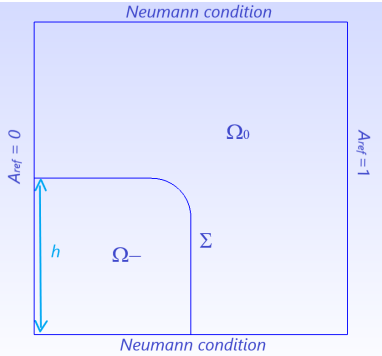

(A) Geometry and boundary conditions.

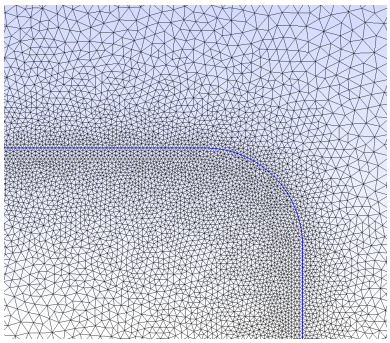

(B) Problem with a fine mesh on the interface Σ.

Parameters	Value
Relative permeability (μ_r)	4000
Conductivity (σ)	2E+06 S/m
Frequency (f)	10 Hz
Conductor height (h)	0.1 m
Skin depth (δ)	1.779E-03 m
Epsilon (ε)	1.41E-01

(C) Physical and numerical parameters.

FIGURE 3. Framework of the problem.

the second order approach solution, we illustrate the isovalues of its corresponding error. Finally, a numerical convergence analysis of our asymptotics and the impedance solution with the Leontovitch condition will be achieved. Some comments will be discussed, especially for the convergence results.

4.1. **Framework.** First, our numerical simulation is based on the finite element approach with a fine mesh on the interface Σ, see for instance Fig. 3 (B). The asymptotic models (8)-(10) are classical and require no special finite element spaces. Therefore, we choose the classical P^2 Lagrange finite elements. We note that the numerical computation is done on the Python interface thanks to the flexible library GetFEM [18]. The physical and numerical parameters used, the geometry and the boundary conditions are depicted in Fig. 3. Here we note that the skin depth is about 17 % of the height h of the domain Ω_-.

4.2. **Numerical experiments.** It is well-known that whenever a conductor is placed in a time-varying magnetic field we get an induced current that concentrates near the surface of the conductor. In addition, at a distance called the skin depth δ the amplitude of the current density vector decreases to $\dfrac{1}{e}$ of its surface value. Actually, this phenomenon is called the *skin effect* and it is depicted in Fig. 4 that illustrates the imaginary part of the reference solution A. Indeed, Fig. 4 shows that the current is restricted to a thin layer near the conductor surface and decreases exponentially with depth.

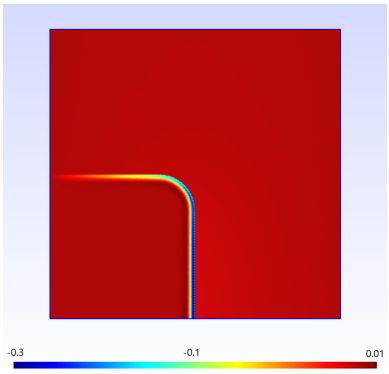

FIGURE 4. Numerical simulation of the skin effect.

Moreover, Fig. 5 (A) reflects the perfect magnetic conductor condition since the magnetic field lines penetrate in an orthogonal way to the conductor Ω_-.

Now we perform post-treatments of our numerical computations in order to investigate the precision of the proposed asymptotic solutions up to the order two in the free space Ω_0. First, we recall that the first asymptotic A_0^+ is a real valued function and presented by its isovalues in Fig. 5 (B). We remark that Fig. 5 (A) corresponding to the real part of the reference solution is

coherent with the Fig. 5 (B). However, this result is not sufficient to prove the good accuracy of the first asymptotic A_0^+, since we are considering only the real part of the reference solution A and the asymptotic A_0^+ as well. For this reason, we exhibit another way to validate our estimation: we make a comparison between the error of the first order $A^+ - A_0^+$ in Ω_0 and its corresponding correction $\frac{\varepsilon}{\alpha}A_1^+$, which are illustrated in Fig. 6 (A)-(B) for the imaginary part. We remark that the two latter figures are approximately the same. Moreover, we note that we have the same results for the real part. As a consequence, we conclude that we have a good correction as well as a good precision of the first asymptotic A_0^+.

Next, the accuracy of the second order approximation $A_0^+ + \frac{\varepsilon}{\alpha}A_1^+$ is evaluated by establishing the corresponding error $A^+ - A_0^+ - \frac{\varepsilon}{\alpha}A_1^+$. The second order error for the real and imaginary parts is less than 2E-04, see Fig. 7 (A)-(B) . We note that the second order error is small enough since it satisfies the optimal estimate (7) defined in Theorem 1. Thus, this result illustrates the good accuracy of the second order parametrization $A_0^+ + \frac{\varepsilon}{\alpha}A_1^+$.

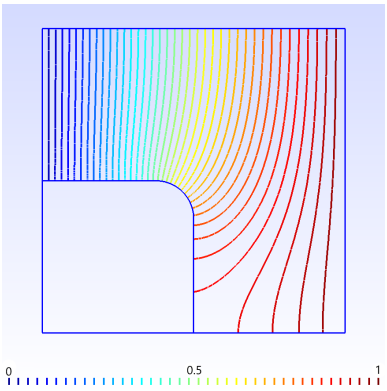

(A) Real part of the reference solution in Ω_0.

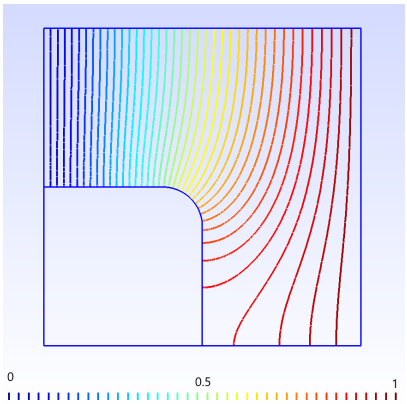

(B) Real part of the first asymptotic A_0^+.

FIGURE 5. Direction of the magnetic field lines

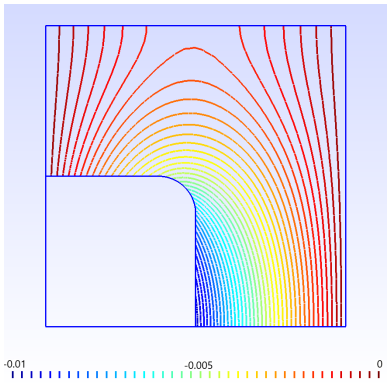

(A) Imaginary part of the error $A^+ - A_0^+$

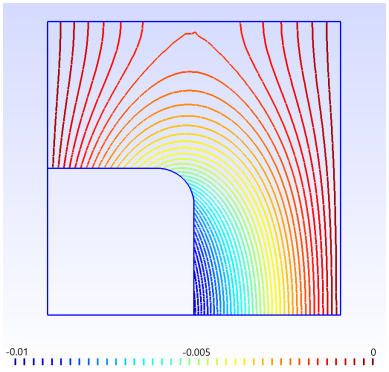

(B) Imaginary part of the correction $\frac{\varepsilon}{\alpha} A_1^+$

FIGURE 6. Error and correction of order one.

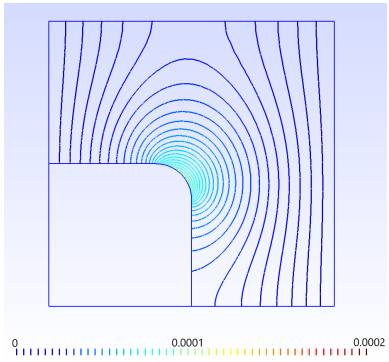

(A) Real part of the error of order 2: $A^+ - A_0^+ - \frac{\varepsilon}{\alpha} A_1^+$

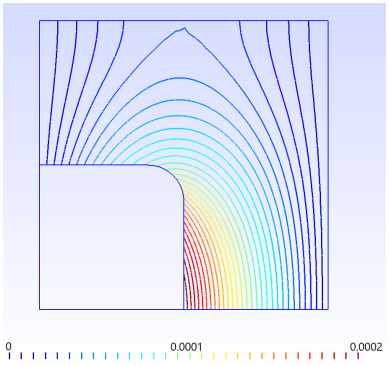

(B) Imaginary part of the error of order 2: $A^+ - A_0^+ - \frac{\varepsilon}{\alpha} A_1^+$

FIGURE 7. Error of order 2.

4.3. **Convergence results.** We recall that the impedance solution with the Leontovitch condition denoted by A_1^ε satisfies the following boundary value problem

$$\begin{cases} -\Delta A_1^\varepsilon = \mu_0 J_s & in \quad \Omega_0 \\ \partial_n A_1^\varepsilon + \dfrac{\varepsilon}{\alpha} A_1^\varepsilon = 0 & on \quad \Sigma \\ A_1^\varepsilon = 0 & on \quad \Gamma. \end{cases} \tag{14}$$

Indeed, it is well known that the Leontovitch solution has a high accuracy with respect to our reference solution A^+[17]. Therefore we intend to compare the performance of the asymptotics up to the order two with the latter impedance solution. In this context, we plot the convergence graphs with the log scale using the following error estimate:

$$\text{Error} = \frac{\sqrt{\int_{\Omega_0} \|\nabla A_{ref} - \nabla A_{num}\|^2 dx}}{\sqrt{\int_{\Omega_0} \|\nabla A_{ref}\|^2 dx}}$$

where A_{ref} denotes the reference solution, and A_{num} is the first order asymptotic model A_0^+, the second order asymptotic model $A_0^+ + \frac{\varepsilon}{\alpha} A_1^+$, or the impedance solution A_1^ε. Moreover, we assume that the relative permeability is restricted between 250 and 16000.

First, Fig. 8 (A) ensures that, when the parameter ε decreases, the error of

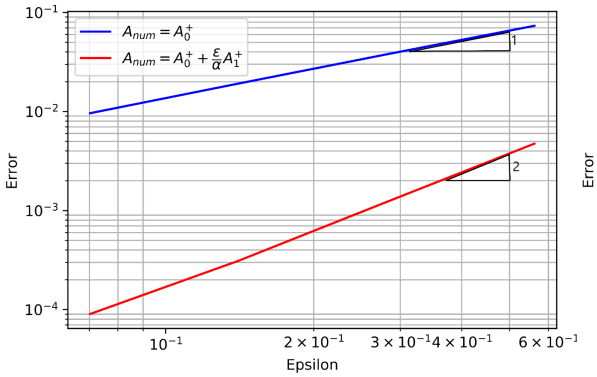

(A) Convergence graphs of the asymptotic solutions of order 1 and 2.

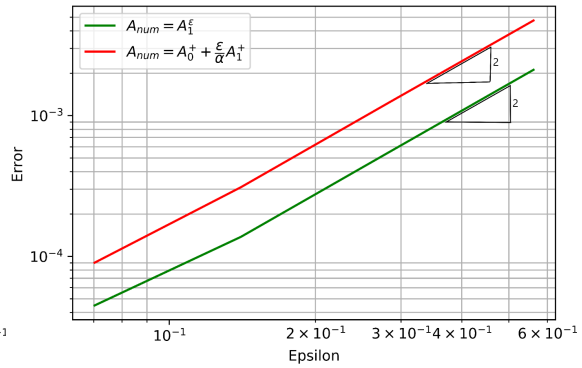

(B) Convergence graphs of the impedance solution A_1^ε and the asymptotic solution of order 2.

FIGURE 8. Convergence results.

order 2 decays more rapidly than the error of order one. Thus the asymptotic solution of order 2 is more accurate than the asymptotic solution of order 1.

On the contrary the red and green curves, exhibited in Fig. 8 (B) and corresponding to the error of order two and the impedance error, behave in a similar manner with the variation of ε. Therefore the asymptotic solution of order two is coherent with the Leontovitch impedance solution.

However we must note that the impedance boundary value problem(14) depend on the parameter ε. As a result, the Leontovitch solution is not more efficient, since at each step we change the frequency, the conductivity as well as the relative permeability, we must compute the finite element method. On the contrary, the asymptotic models need to be computed only once since it does not depend on any physical parameter, see problems (8)-(10).

Finally, the convergence results exhibited in Fig. 8 (A), for the considered non smooth domain (see Fig. 3 (A)), coincides with the theoretical studies introduced in the section 3.1.

5. Conclusion and perspectives

We evaluated the performance of the asymptotic models up to the order two using a finite element approach with a fine mesh on the interface of the conductor. We have been able to establish the modeling and the numerical simulation of the magnetic skin effect. We obtained also that the computational costs of the asymptotic solution of order two is less than the impedance solution with the Leontovitch condition regardless the number of the physical parameters to be considered. Finally, our numerical experiments are in accordance with the theoretical studies concerning the convergence results.

Future works will investigate higher order asymptotic models as well as 3D structures of the eddy current problems for ferromagnetic materials.

Appendix A. Elements of derivation for the multiscale expansion

We assume that Σ is a smooth curve of length L. We remind that the magnetic vector potential decays rapidly with depth inside the conductor. Therefore it is beneficial to derive a multiscale expansion for the solution inside the conductor. In order to perform this approach, we define a tubular neighborhood $\nu(\Sigma)$ of Σ of a small parameter $h_0 > 0$ in the inner domain Ω_- as follows

$$\nu(\Sigma) = \{\mathbf{x}(\xi, h) = \mathbf{X}(\xi) + hn(\xi), (\xi, h) \in \Sigma \times (0, h_0)\}$$

see for instance Notation(2). For $h_0 < \dfrac{1}{\|k\|_\infty}$, we introduce the change of coordinates

$$\Psi : \mathbf{x} = (x, y) \longmapsto (\xi, h)$$

from $\nu(\xi)$ into the cylinder $\mathbb{T}_L \times (0, h_0)$ (see Notation(2)).

The following sections are dedicated to identify the profiles $\mathcal{U}_n$ as well as the asymptotic models in the free space at any order $n \in \mathbb{N}$. Let us first expand the Laplace operator Δ and the normal partial derivative ∂_n in power series of the skin depth δ by applying the change of variables Ψ and the scaling $Y = \dfrac{h}{\delta}$. Then we insert the resulting expression in the equations of the problem (3). Finally, by identifying with the same power in ε, δ and μ_r, we get the coefficients of the asymptotic expansion satisfying a family of boundary value problems at any order $n \in \mathbb{N}$. For the sake of simplicity, we will explicit the first asymptotics $\mathcal{U}_n$ and A_n^+ for $n = 0, 1, 2$ by induction.

A.1. **Expansion of the operators in power series of δ.** Performing the change of variables Ψ, the Laplace operator writes in coordinates (ξ, h) as

$$\Delta = Q^{-1}[\partial_h(Q\partial_h) + \partial_\xi(Q^{-1}\partial_\xi)] \tag{15}$$

where $Q = (1 - hk(\xi))$. We then apply the scaling

$$Y = \frac{h}{\delta}$$

in order to make appear the small parameter δ in (15). Therefore this operator expands in power series of δ as follows

$$\delta^2\Delta = \partial_Y^2 + \sum_{n\geq 1}\delta^n A_n$$

Observe that

$$\begin{array}{c} A_1 = -k(\xi)\partial_Y, \\ A_2 = \partial_\xi^2 - k(\xi)^2 Y\partial_Y. \end{array} \tag{16}$$

Similarly, we write

$$\partial_n(\xi;\partial_Y) = \frac{1}{\delta}\partial_Y$$

on the interface Σ.

A.2. **Equations of the coefficients of the magnetic potential.** In this section we define $v_\delta(\xi, Y) = A^-(\mathbf{x})$ in $\nu(\Sigma)$. After the scaling $h \longmapsto Y = \dfrac{h}{\delta}$ in $\nu(\Sigma)$, the problem(3) writes

$$\left\{\begin{array}{lll} -\Delta A^+ = \mu_0 J & in & \Omega_0, \\ \partial_n A^+ = \varepsilon\partial_Y v_\delta & on & \Sigma, \\ A^+ = 0 & on & \Gamma, \end{array}\right. \tag{17}$$

and

$$\left\{\begin{array}{lll} (-\partial_Y^2 + (\frac{1}{\alpha})^2)v_\delta - \sum\limits_{n\geq 1}\delta^n A_n v_\delta = 0 & in & \mathbb{T}_L \times (0,+\infty), \\ v_\delta = A^+ & on & \mathbb{T}_L \times \{0\}, \end{array}\right. \tag{18}$$

Now we insert the ansatz

$$A^+ \sim \sum_{n\geq 0}(\frac{\varepsilon}{\alpha})^n A_n^+(\mathbf{x}) \quad in \quad \Omega_0, \qquad and \qquad v_\delta \sim \sum_{n\geq 0}\delta^n \mathcal{U}_n(\xi, Y) \quad in \quad \nu(\Sigma) \tag{19}$$

with $\mathcal{U}_n(., Y) \longmapsto 0$ as $Y \longmapsto \infty$, in equations (17) and (18). Then by identification of terms with the same powers of ε, δ and μ_r, the profiles $\mathcal{U}_n$ and A_n^+ satisfy the following family of problems coupled by their conditions on the interface Σ

$$\left\{\begin{array}{lll} -\Delta A_n^+ = \mu_0 J\delta_n^0 & in & \Omega_0, \\ \partial_n A_n^+ = \alpha^n(\delta_0^2)^{n-1}\partial_Y \mathcal{U}_{n-1} & on & \Sigma, \\ A_n^+ = 0 & on & \Gamma, \end{array}\right. \tag{20}$$

and

$$\left\{\begin{array}{lll} -\partial_Y^2\mathcal{U}_n + (\frac{1}{\alpha})^2\mathcal{U}_n = \sum\limits_{p=1}^{n} A_p\mathcal{U}_{n-p} & in & \Sigma \times (0,+\infty), \\ \mathcal{U}_n = (\frac{1}{\alpha\delta_0^2})^n A_n^+ & on & \Sigma, \end{array}\right. \tag{21}$$

where $\delta_0 = \sqrt{\frac{2}{\omega\sigma\mu_0}}$. In (20) δ_n^0 denotes the Kronecker symbol and we use the convention $\mathcal{U}_{-1} = 0$. In the next section we make explicit the first asymptotics $\mathcal{U}_n$ and A_n^+ for $n = 0, 1, 2$ by induction.

A.3. **First terms of the asymptotics for the magnetic potential.** For n=0, we obtain from (20) that A_0^+ solves the problem below

$$\left\{\begin{array}{lll} -\Delta A_0^+ = \mu_0 J & in & \Omega_0, \\ \partial_n A_0^+ = 0 & on & \Sigma, \\ A_0^+ = 0 & on & \Gamma. \end{array}\right. \tag{22}$$

Then according to (20) $\mathcal{U}_0$ solves the ODE below

$$\left\{\begin{array}{ll} -\partial_Y^2 \mathcal{U}_0 + (\frac{1}{\alpha})^2 \mathcal{U}_0 = 0 & in \quad \Sigma \times (0, +\infty), \\ \mathcal{U}_0 = A_0^+ & on \quad \Sigma. \end{array}\right. \tag{23}$$

The unique solution of (23) such that with $\mathcal{U}_0 \longrightarrow 0$ as $Y \longrightarrow \infty$, is

$$\mathcal{U}_0(\xi, Y) = A_0^+(\mathbf{X}(\xi)) e^{-\frac{Y}{\alpha}}. \tag{24}$$

Next, for $n = 1$, we determine A_1^+ according to (24) that solves

$$\left\{\begin{array}{lll} -\Delta A_1^+ = 0, & in & \Omega_0, \\ \partial_n A_1^+ = -A_0^+ & on & \Sigma, \\ A_1^+ = 0 & on & \Gamma. \end{array}\right. \tag{25}$$

Then, according to (25), $\mathcal{U}_1$ solves the following ODE

$$\left\{\begin{array}{ll} -\partial_Y^2 \mathcal{U}_1 + (\frac{1}{\alpha})^2 \mathcal{U}_1 = \frac{1}{\alpha} k(\xi) A_0^+ & in \quad \Sigma \times (0, +\infty), \\ \mathcal{U}_1 = \frac{1}{\alpha\delta_0^2} A_1^+(\mathbf{X}(\xi)) & on \quad \Sigma. \end{array}\right. \tag{26}$$

The unique solution of (26) such that $\mathcal{U}_1 \longrightarrow 0$ as $Y \longrightarrow \infty$ is

$$\mathcal{U}_1(\xi, Y) = \left(\frac{1}{\alpha\delta_0^2} A_1^+(\mathbf{X}(\xi)) + \frac{k(\xi)}{2} A_0^+(\mathbf{X}(\xi)) Y \right) e^{-\frac{Y}{\alpha}}. \tag{27}$$

Next, We determine the third term A_2^+. According to (20) for $n = 2$ and (27, A_2^+ solves the following problem

$$\left\{\begin{array}{lll} -\Delta A_2^+ = 0 & in & \Omega_0, \\ \partial_n A_2^+ = \dfrac{k(\xi)}{2} A_0^+ - \dfrac{1}{\alpha^2\delta_0^2} A_1^+ & on & \Sigma, \\ A_2^+ = 0 & on & \Gamma. \end{array}\right. \tag{28}$$

Finally, according to (28), $\mathcal{U}_2$ solves the following ODE

$$\left\{\begin{array}{ll} -\partial_Y^2 \mathcal{U}_2 + (\frac{1}{\alpha})^2 \mathcal{U}_2 = -k(\xi)\partial_Y \mathcal{U}_1 + A_2 \mathcal{U}_0 & in \quad \Sigma \times (0, +\infty), \\ \mathcal{U}_2 = (\frac{1}{\alpha\delta_0^2})^2 A_2^+(\mathbf{X}(\xi)) & on \quad \Sigma. \end{array}\right. \tag{29}$$

According to (27), we can explicit the right-hand side of this ODE

$$\partial_Y \mathcal{U}_1 = \left(\frac{k(\xi)}{2} A_0^+ - \frac{1}{\alpha} \left(\frac{\delta_0}{\alpha} A_1^+ + \frac{k(\xi)}{2} A_0^+ Y \right) \right) (X(\xi)) e^{-\frac{Y}{\alpha}}$$

and according to $(16)_2$ and (24) we infer successively

$$A_2\mathcal{U}_0(\xi,Y)=\{\partial_\xi^2-k(\xi)^2Y\partial_Y\}\mathcal{U}_0(\xi,Y)=(\partial_\xi^2A_0^+-\frac{1}{\alpha}k(\xi)^2YA_0^+)(X(\xi))e^{-\frac{Y}{\alpha}}.$$

Then, the unique solution of the ODE (29) such that $\mathcal{U}_2\longrightarrow 0$ as $Y\longrightarrow\infty$ is

(30)
$$\mathcal{U}_2(\xi,Y)=\left(\left(\frac{1}{\alpha\delta_0^2}\right)^2A_2^+-\left(\frac{k(\xi)}{2}\frac{\delta_0}{\alpha}A_1^+-\frac{\alpha}{2}\left\{\partial_\xi^2-\frac{k(\xi)^2}{4}\mathbb{I}\right\}A_0^+\right)Y-\frac{3k(\xi)^2}{8}A_0^+Y^2\right)(X(\xi))e^{-\frac{Y}{\alpha}}.$$

Remark 1. *The asymptotic models presented above can be deduced directly from* [17]. *Indeed, in* [17], *we developed* $\tilde{\varepsilon}-$*parametrization for the magnetic potential* A *where* $\tilde{\varepsilon}=\dfrac{1}{\sqrt{\mu_r}}$. *We recall the asymptotic expansions of the magnetic potential in* [17] *(cf (2.10)-(2.11)-(2.12))*

$$A^+(\boldsymbol{x})=\mathcal{A}_0^+(\boldsymbol{x})+\tilde{\varepsilon}\mathcal{A}_1^+(\boldsymbol{x})+\tilde{\varepsilon}^2\mathcal{A}_2^+(\boldsymbol{x})+\cdots\qquad in\quad\Omega_0, \tag{31}$$

$$A^-(\boldsymbol{x})=\mathbb{U}_0(\xi,\tilde{Y})+\tilde{\varepsilon}\mathbb{U}_1(\xi,\tilde{Y})+\tilde{\varepsilon}^2\mathbb{U}_2^+(\xi,\tilde{Y})+\cdots\qquad in\quad\Omega_-, \tag{32}$$

where $\mathbb{U}_j(.,\tilde{Y})\longrightarrow 0$ *when* $\tilde{Y}=\dfrac{h}{\tilde{\varepsilon}}\longrightarrow\infty,\forall j\in\mathbb{N}$, *and* (ξ,h) *is a curvilinear coordinate system (see for instance Fig. 2). Now the asymptotic expansions (4)-(5) of the present work can be written as follows*

$$A^+(\boldsymbol{x})=A_0^+(\boldsymbol{x})+\tilde{\varepsilon}\frac{1}{\delta_0\alpha}A_1^+(\boldsymbol{x})+\tilde{\varepsilon}^2\Big(\frac{1}{\delta_0\alpha}\Big)^2A_2^+(\boldsymbol{x})+\cdots\qquad in\quad\Omega_0, \tag{33}$$

$$A^-(\boldsymbol{x})=\mathcal{U}_0(\xi,\frac{h}{\delta})+\tilde{\varepsilon}\delta_0\mathcal{U}_1(\xi,\frac{h}{\delta})+\tilde{\varepsilon}^2\delta_0^2\mathcal{U}_2(\xi,\frac{h}{\delta})+\cdots\qquad in\quad\Omega_-, \tag{34}$$

where $\delta_0=\sqrt{\dfrac{2}{\omega\sigma\mu_0}}$, *and* $\mathcal{U}_j(.,Y)\longrightarrow 0$ *when* $Y=\dfrac{h}{\delta}\longrightarrow\infty,\forall j\in\mathbb{N}$. *Observe that from the above asymptotic expansions, we deduce the following relations*

- *In* Ω_0, *we get*

$$\begin{cases}\mathcal{A}_0^+(\boldsymbol{x})=A_0^+(\boldsymbol{x}),\\ \mathcal{A}_1^+(\boldsymbol{x})=\dfrac{1}{\delta_0\alpha}A_1^+(\boldsymbol{x}),\\ \mathcal{A}_2^+(\boldsymbol{x})=\dfrac{1}{\delta_0^2\alpha^2}A_2^+(\boldsymbol{x}).\end{cases} \tag{35}$$

- *In* Ω_-, *we get*

$$\begin{cases}\mathbb{U}_0(\xi,\tilde{Y})=\mathcal{U}_0(\xi,Y),\\ \mathbb{U}_1(\xi,\tilde{Y})=\delta_0\mathcal{U}_1(\xi,Y),\\ \mathbb{U}_2(\xi,\tilde{Y})=\delta_0^2\mathcal{U}_2(\xi,Y).\end{cases} \tag{36}$$

Finally, we conclude directly from the asymptotic expressions in [17] *(section 6.3), our asymptotic models (22)-(24)-(25)-(27)-(28)-(30).*

References

[1] X. Antoine, H. Barucq, and L. Vernhet. High-frequency asymptotic analysis of a dissipative transmission problem resulting in generalized impedance boundary conditions. *Asymptotic Analysis*, 26(3, 4):257–283, 2001.

[2] A. Bossavit. Électromagnétisme, en vue de la modélisation, volume 14 of mathématiques & applications (berlin)[mathematics & applications]. *Springer-Verlag, Paris*, 201:202, 1993.

[3] A. Buffa, H. Ammari, and J.-C. Nédélec. A justification of eddy currents model for the maxwell equations. *SIAM Journal on Applied Mathematics*, 60(5):1805–1823, 2000.

[4] M. Costabel, M. Dauge, and S. Nicaise. Singularities of eddy current problems. *ESAIM: Mathematical Modelling and Numerical Analysis*, 37(5):807–831, 2003.

[5] H. Haddar, P. Joly, and H.-M. Nguyen. Generalized impedance boundary conditions for scattering by strongly absorbing obstacles: the scalar case. *Mathematical Models and Methods in Applied Sciences*, 15(08):1273–1300, 2005.

[6] R. Hiptmair. Symmetric coupling for eddy current problems. *SIAM Journal on Numerical Analysis*, 40(1):41–65, 2002.

[7] N. Ida and S. Yuferev. Impedance boundary conditions for transient scattering problems. *IEEE Transactions on Magnetics*, 33(2):1444–1447, 1997.

[8] M. Issa, J.-R. Poirier, R. Perrussel, O. Chadebec, and V. Péron. Boundary element method for 3d conductive thin layer in eddy current problems. *COMPEL-The international journal for computation and mathematics in electrical and electronic engineering*, 38(2):502–521, 2019.

[9] L. Krähenbühl, P. Dular, V. Péron, R. Perrussel, R. V. Sabariego, and C. Poignard. Efficient delta-parametrization of 2d surface-impedance solutions. *Proceedings of COMPUMAG 2015*, page 2, 2015.

[10] L. Krahenbuhl and D. Muller. Thin layers in electrical engineering-example of shell models in analysing eddy-currents by boundary and finite element methods. *IEEE Transactions on Magnetics*, 29(2):1450–1455, 1993.

[11] L. Krähenbühl, V. Péron, R. Perrussel, and C. Poignard. *On the asymptotic expansion of the magnetic potential in eddy current problem: a practical use of asymptotics for numerical purposes*. PhD thesis, INRIA Bordeaux; INRIA, 2015. `https://hal.inria.fr/hal-01174009`.

[12] R.C. MacCamy and E. Stephan. Solution procedures for three-dimensional eddy current problems. *Journal of mathematical analysis and applications*, 101(2):348–379, 1984.

[13] R.C. Maccamy and E. Stephan. A skin effect approximation for eddy current problems. *Archive for Rational Mechanics and Analysis*, 90(1):87–98, 1985.

[14] I. D. Mayergoyz and G. Bedrosian. On calculation of 3-d eddy currents in conducting and magnetic shells. *IEEE Transactions on Magnetics*, 31(3):1319–1324, 1995.

[15] V. Péron. Asymptotic expansion for the magnetic potential in the eddy current problem: the ferromagnetic case. 2015. `https://hal.inria.fr/hal-01253971`.

[16] V. Péron. Asymptotic models and impedance conditions for highly conductive sheets in the time-harmonic eddy current model. *SIAM Journal on Applied Mathematics*, 79(6):2242–2264, 2019.

[17] V. Péron and C. Poignard. On a magnetic skin effect in eddy current problems: the magnetic potential in magnetically soft materials. *Zeitschrift für angewandte Mathematik und Physik*, 72(4):1–19, 2021. `https://doi.org/10.1007/s00033-021-01596-6`.

[18] Y. Renard and K. Poulios. Getfem: Automated fe modeling of multiphysics problems based on a generic weak form language. *ACM Transactions on Mathematical Software (TOMS)*, 47(1):1–31, 2020. `https://hal.archives-ouvertes.fr/hal-02532422/document`.

[19] A Alonso Rodríguez, P. Fernandes, and A. Valli. Weak and strong formulations for the time-harmonic eddy-current problem in general multi-connected domains. *European Journal of Applied Mathematics*, 14(4):387–406, 2003.
[20] K. Schmidt and A. Chernov. A unified analysis of transmission conditions for thin conducting sheets in the time-harmonic eddy current model. *SIAM Journal on Applied Mathematics*, 73(6):1980–2003, 2013.

Dima Abou El Nasser El Yafi
Laboratoire de mathématiques appliquées de Pau, E2S UPPA, CNRS
Université de Pau et des pays de l'Adour
64000 Pau
France
E-mail: dima.abou-el-nasser-el-yafi@univ-pau.fr

Victor Péron
Laboratoire de mathématiques appliquées de Pau, E2S UPPA, CNRS
Université de Pau et des pays de l'Adour
64000 Pau
France
E-mail: victor.peron@univ.pau.fr

Ronan Perrussel
LAPLACE, CNRS, INPT, UPS
Université de Toulouse
Toulouse
France
E-mail: ronan.perrussel@laplace.univ-tlse.fr

Laurent Krähenbühl
CNRS, ECL, UCBL, INSA Lyon, Ampère(UMR5005)
Université de Lyon
69130 Ecully
France
E-mail: laurent.krahenbuhl@ec-lyon.fr